

Issam Mudawar
Professor and Director.

Peter E. Jimenez
Graduate Student.

Electronic Cooling Research Center,
Boiling and Two-Phase Flow Laboratory,
School of Mechanical Engineering,
Purdue University,
West Lafayette, IN 47907-1288

Robert E. Morgan

Lead Technologist for
Advanced Materials/Avionics,
Naval Air Warfare Center,
Aircraft Division Indianapolis,
Indianapolis, IN 46219-2189

Immersion-Cooled Standard Electronic Clamshell Module: A Building Block for Future High-Flux Avionic Systems

An 820-Watt clamshell module was fabricated and tested in order to assess the feasibility of cooling future high heat flux avionic hardware via subcooled phase change. One half of the module was constructed from aluminum 7075-T6 and populated with 16 heat sources simulating microelectronic chips. The other half was substituted with a transparent plastic cover to facilitate optical access to the boiling taking place in the module cavity. A dielectric coolant, Fluorinert FC-72, was supplied to, and rejected from the module via sleeveless quick connection couplers. Tests were performed with an inlet coolant pressure of 1.52 bar (22 psia) and inlet temperatures ranging from 27 to 47°C. These tests yielded power dissipation exceeding 410 W per half module for coolant flow rates and pressure drops as small as 0.023 kg/s (0.221 gpm) and 0.149 bar (2.16 psia), respectively, and the device and rib guide temperatures were maintained below 80 and 60°C, respectively. The pressure drop remained constant with increasing module power proving, as was confirmed visually, it is possible to condensate all the vapor within the module cavity, allowing only liquid to exit the module. Thus, coolant conditioning external to the module can be greatly simplified by employing a simple single-phase liquid flow loop.

1 Introduction

Since the introduction of the silicon integrated circuit, there has been a continuing trend of miniaturization of integrated circuit feature size, which is currently smaller than 0.025 microns for silicon MOSFETS. These technological advances, aided, in part, by an increase in chip size, have made possible an excess of five orders-of-magnitude increase in the number of components integrated in a single chip. The quest for greater functionality per unit area has also driven the industry to squeeze a large number of chips on a single board. This ever increasing rate of integration has led to alarming increases in heat dissipation in many cutting-edge commercial and military electronic technologies.

Thermal management is a primary design need in modern electronic packaging for both military and commercial systems. High temperature environments and excessive heat induce high failure rates and unacceptable reliability. Regardless of the thermal environment, electronic device junctions must be maintained at temperature levels consistent with performance and reliability objectives. Passive conduction/convection techniques, applicable to low power electronics of the past three decades, are no longer suitable for the higher thermal densities now encountered and coming in future systems.

To meet the high performance needs for future electronic systems, Navy and Air Force programs have been investigating and developing techniques and standardized hardware for enhanced electronic packaging. Two well-known programs are the Standard Electronic Module (SEM) program and the Joint Integrated Avionics Working Group (JIAWG). Advanced fixed and rotary winged platforms now in development are experiencing nearly an order-of-magnitude increase (200 to 300 W for SEM-E format modules) in power/cooling requirements. The trend for increased power density and severe operating environments will continue as space and weight constraints become more critical; thus, the need for highly efficient thermal management systems that meet power dissipation and complex physical integration constraints.

An example of the on-going efforts to enhance electronic systems is the Air Force Pave program initiated in 1990 to develop standard modular avionics for future aircraft. About one half of the close to 200 SEM-E modules identified for future aircraft systems dissipate less than 40 W and could, therefore, be easily cooled with conventional passive (i.e., conduction) cooling. However, some of the modules, especially the integrated core processors, produce well in excess of 40 W (Mackowski, 1991).

Thermal management in most of today's SEM-E format modules consists of a conduction/convection scheme that conducts the heat away from the device through a thermal bridge consisting of a solder layer, a multi-layer circuit board, card

Contributed by the Electrical and Electronic Packaging Division for publication in the JOURNAL OF ELECTRONIC PACKAGING. Manuscript received by the EEPD April 1, 1993; revised manuscript received December 16, 1993. Associate Technical Editor: B. G. Sammakia.

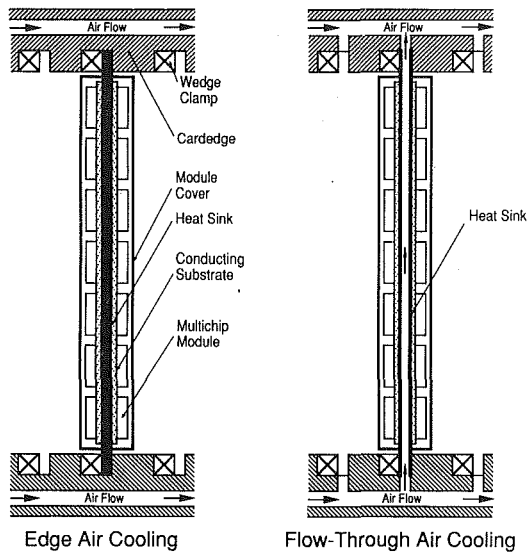


Fig. 1(a, b)

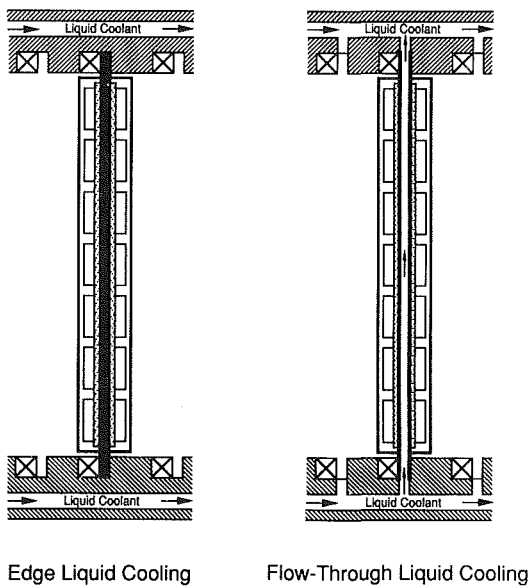
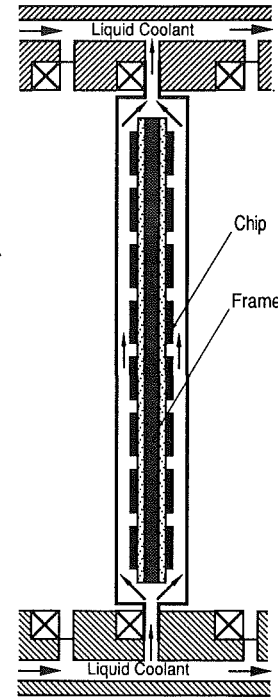


Fig. 1(c, d)



Liquid Immersion Cooling

Fig. 1(e)

Fig. 1 Avionic cooling schemes featuring (a) conduction cooled center frame (heat sink) module clamped to air cooled cardcage rail, (b) air flow-through center frame module, (c) conduction cooled center frame module clamped to liquid cooled cardcage rail, (d) liquid flow-through center frame module, and (e) liquid immersion chip-on-board module

rails and a compact heat exchanger which rejects the heat to air bled from the compressor of the aircraft engine as illustrated in Fig. 1(a). The main drawback to this edge air cooling technique is its relatively large thermal resistance which precludes the use of this passive cooling configuration with modules dissipating more than about 40 W. Some improvement in cooling rate is possible by supplying air through the module itself, Fig. 1(b). Further improvement can also be achieved with liquid cooling along the edge of the board, Fig. 1(c), or through the

Nomenclature

A_{chip} = surface area of chip
 c_p = specific heat at constant pressure
 g = gravitational acceleration
 h_{fg} = latent heat of vaporization
 \dot{m}_{hmod} = mass flow rate of half module (test module)
 \dot{m}_{mod} = mass flow rate of clamshell module
 N = number of chips per module
 p = pressure
 Δp = pressure drop across clamshell module
 q'' = chip heat flux based on $12.7 \times 12.7 \text{ mm}^2$ surface area
 q_{hmod} = heat dissipation rate per half module (test module)
 q_{mod} = heat dissipation rate of clamshell module
 q_m'' = critical heat flux based on $12.7 \times 12.7 \text{ mm}^2$ surface area
 T = temperature
 T_f = liquid temperature
 ΔT_{sub} = liquid subcooling, $T_{\text{sat}} - T_f$

ΔT_w = temperature difference between chip surface and liquid inlet, $T_w - T_i$
 TC = thermocouple
 x_e = thermodynamic equilibrium quality at module exit
 ρ = density
 σ = surface tension

Subscripts

chip = chip
 e = module exit
 f = liquid
 g = vapor
 guide = guide rib
 hmod = half module
 i = module inlet
 mod = module
 sat = saturation
 sub = subcooling
 w = chip surface condition.

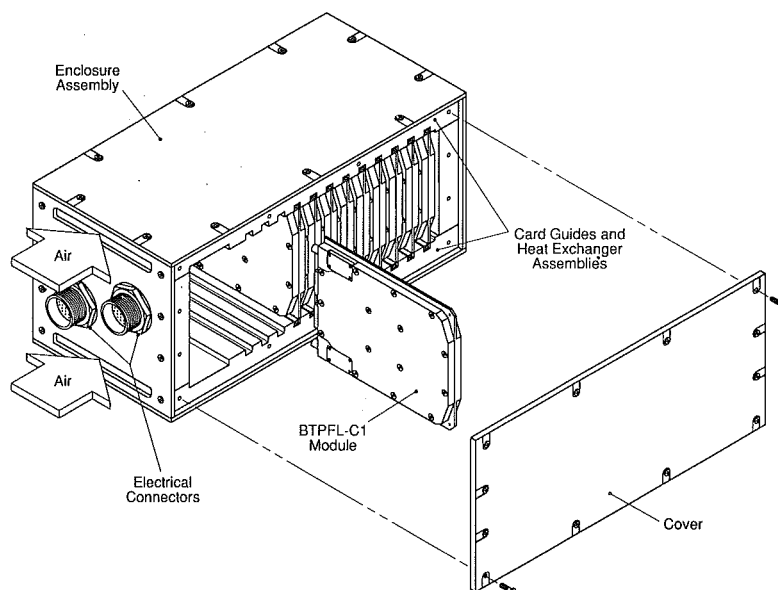


Fig. 2 BTPFL-C1 clamshell modules inserted in a standard avionic enclosure

module, Fig. 1(d). But best results are attained when a liquid coolant is brought in direct contact with the device itself, Fig. 1(e).

The Pave Pace program yielded a new building block for high power aircraft avionics which is comparable with conventional SEM-E circuit boards and connector requirements (Barwick et al., 1991). Using the configuration illustrated in Fig. 1(d), cooling was achieved via a liquid flow-through aluminum frame onto which the devices could be bonded, bringing the coolant to within a few millimeters of the device. This frame featured a sleeveless, drip-free quick connection liquid couplers with an outer envelope smaller than 1.52 cm (0.6 in). Using polyalphaolefin (PAO) as coolant, the frame yielded a cooling rate of 200 W at a device junction temperature smaller than 85°C. While further improvement in the thermal performance of the liquid flow-through frame is underway, limitations on the convective heat transfer coefficient of liquid flow and the relatively large pressure drop associated with the drastic increase in liquid viscosity at sub-zero ambient temperatures place an upper bound of approximately 250 W on its cooling rate.

It is apparent from the trends in avionics packaging during the past two decades that new thermal management technologies had to be continually developed or existing ones updated in response to the increases in heat dissipation. What has been lacking, thus far, is a cooling technology which would not only satisfy the stringent cooling demands of near-term high heat flux devices, but would continue to meet these requirements amidst the ongoing trend of increasing heat dissipation.

The last decade witnessed the development of many innovative approaches to cooling high-flux electronic hardware. These include enhanced pool boiling (Nakayama et al., 1984; Anderson and Mudawar, 1989; Mudawar and Anderson, 1990), flow boiling (Maddox and Mudawar, 1989; Mudawar and Maddox, 1989, 1990), falling films (Grimley et al., 1988), jet impingement (Monde and Katto, 1978; Ma and Bergles, 1983; Wadsworth and Mudawar, 1990, 1992), curved flow (Galloway and Mudawar, 1992), and microchannels (Tuckerman and Pease, 1981; Phillips, 1988; Bowers and Mudawar, 1993). Key to enhancing cooling effectiveness in most of these approaches has been the direct (immersion) cooling of the device with a dielectric liquid. Intimate contact between the coolant and the device greatly reduces the overall thermal resistance between the device and the ultimate coolant (e.g., air from the com-

pressor), allowing the device to dissipate very high fluxes while maintaining a relatively low junction temperature. Heat transfer from the device can also be greatly ameliorated by allowing the liquid to undergo change of phase. The rapid growth and departure of minute vapor bubbles due to evaporation of liquid on the device surface takes the form of miniature, yet powerful "micro-pumps" which greatly enhance cooling effectiveness, producing only modest increases in device temperature corresponding to enormous increases in heat flux, which is the key advantage of phase-change immersion cooling over other cooling schemes. Using directed, high-speed coolant impingement, phase change facilitated the dissipation of an excess of 660 W from a single 12.7 mm × 12.7 mm chip (Wadsworth and Mudawar, 1992).

Recognizing the merits of subcooled immersion cooling with phase change, the present work was initiated by the U.S. Navy with the aim of building and testing a 1.509 cm (0.594 in) thick immersion cooling clamshell module compatible with existing avionics enclosure packaging constraints. Key requirements in the design of the clamshell module were to house two circuit boards inside the module cavity totally submerged in dielectric liquid, and dissipate in excess of 250 W per board (i.e., 500 W per module). While this cooling rate is well within the capabilities of many existing phase-change immersion cooling techniques, stringent constraints were imposed by the Navy on the coolant flow rate and pressure drop which, along with the geometrical constraints, rendered impractical the adaptation of most of these techniques. This paper will define the key constraints in the design of the clamshell module, provide a description of the module design and construction, detail the heat transfer correlations used in the thermal design, and summarize the test results.

2. BTPFL-C1 Clamshell Module

Packaging Concept. Figure 2 shows clamshell modules mounted side by side in an avionic enclosure. The modules are secured by wedge clamps (see Fig. 1) which provide the required pressure for both fluid and electrical coupling of the clamshell module with mating hardware in the enclosure backboard. Some space is required for the coolant pump and reservoir either within the enclosure itself, as shown in Fig. 2, or in a separate chamber external to the enclosure. Heat is rejected

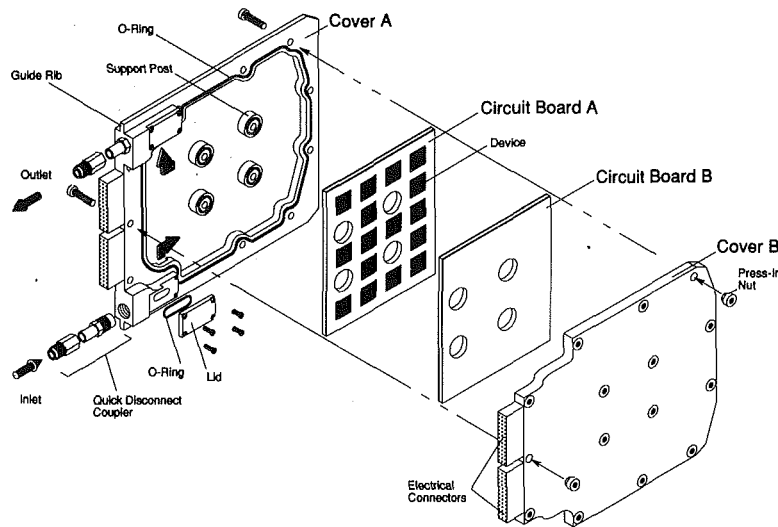


Fig. 3 Construction of the BTPFL-C1 clamshell module

from the module fluid to the compressor air via heat exchanger assemblies located in the top and bottom walls of the enclosure.

Figure 3 shows the asymmetric construction of the BTPFL-C1 clamshell module which houses two circuit boards facing one another inside the module cavity. The module consists of two covers, one of which accommodating both of the fluid couplers. The protrusions in the corners of cover A make available the entire module thickness for mounting the couplers while allowing the module covers to be sealed along the same plane half-way across the module. The liquid coolant is introduced into the module cavity via a slot in one of the coupler protrusions and exits the cavity through an identical slot machined in the other protrusion. Support posts are located in the central region of the module to ensure structural integrity.

Key design requirements for the BTPFL-C1 are summarized in Table 1. These requirements include minimizing coolant flow rate and pressure drop, maintaining the device and rib-guide temperature below 125 and 85 °C, respectively, and limiting coolant interfacing to two sleeveless, drip-free quick connection couplers having an outer envelope smaller than the total module thickness. The unique coupler requirements of the BTPFL-C1 were found to be satisfied with each of three types of miniature couplers manufactured by Hydraflow, Aeroquip and Symetrics. The couplers used in the clamshell module were the Hydraflow DC2004.

Another important objective in designing the clamshell module was to ensure that all the vapor produced in the module cavity condense prior to exiting the module, thus simplifying the coolant conditioning flow loop external to the module.

The large area of the module cavity created potential structural problems such as cover bending and the possibility of exceeding the yield strength of the cover material due to cavity pressure. Therefore, a key consideration in the design of the clamshell module was to use the minimum wall thickness (i.e., minimum weight) possible while ensuring an adequate factor of safety on the wall stresses. This task is complicated by the relatively small overall module thickness, 1.509 cm (0.594 in), and need to maximize the thickness of the module cavity for housing the devices and circuit boards. These constraints dictated that, in addition to the support provided by screws along the module edges, support screws be placed across the module cavity to prevent ballooning or potential rupture of the walls. Despite its relatively poor corrosion resistance, aluminum alloy 7075-T6 was preferred to other aluminum alloys due to its superior yield strength and excellent machinability, and since resistance to corrosion could be easily corrected by anodization.

Table 1 BTPFL-C1 design requirements

	Constraints
Geometrical envelope	<ul style="list-style-type: none"> Module thickness: 1.509 cm (0.594 in) Module height: 13.665 cm (5.380 in), 14.935 cm (5.880 in) rib-to-rib Module width: 16.281 cm (6.410 in) Module cavity: maximize volume for placement of devices
Thermal	<ul style="list-style-type: none"> One half module should dissipate in excess of 250 W Device temperature must not exceed 125 °C Guide rib temperature must not exceed 85 °C
Coolant	<ul style="list-style-type: none"> Dielectric, preferably a 3M Fluorinert Should leave no residue on devices or any other surface it comes in contact with
Pressure	<ul style="list-style-type: none"> Minimize operating pressure inside the module Minimize pressure drop across the module
Flow rate	<ul style="list-style-type: none"> Minimize but maintain above the value corresponding to zero thermodynamic equilibrium quality
Fluid couplers	<ul style="list-style-type: none"> Sleeveless Both parts of coupler should be valved individually to minimize fluid loss during engagement and disengagement of the module Spillage must be less than $1.64 \times 10^{-7} \text{ m}^3$ at pressures ranging from one half to twice the inlet operating pressure
Clamshell material	<ul style="list-style-type: none"> Light weight Corrosion resistant material or aluminum alloy with anodic or chromate coating

Thermal Design of Clamshell Module. Ensuring the complete condensation of the vapor prior to exiting the module was an important objective in designing the clamshell module. This objective was accomplished by supplying the coolant at a temperature much lower than the saturation temperature corresponding to the inlet operating pressure. This subcooling effect provide numerous practical advantages to avionic cooling such as increasing the upper limit on nucleate boiling heat flux, decreasing sensitivity of the boiling process to fluctuations in body force, eliminating the need for a condenser and two-phase coolant reservoir external to the modules, and greatly reducing coolant inventory requirements aboard the aircraft.

The advantages of subcooled boiling are well documented in several previous electronic cooling studies. Maddox and Mudawar (1989) observed that subcooling substantially reduced both the bubble departure diameter and the thickness of the bubble layer. They demonstrated a large degree of subcooling significantly ameliorated critical heat flux (CHF) from an isolated chip. The thinning effect of subcooling on the

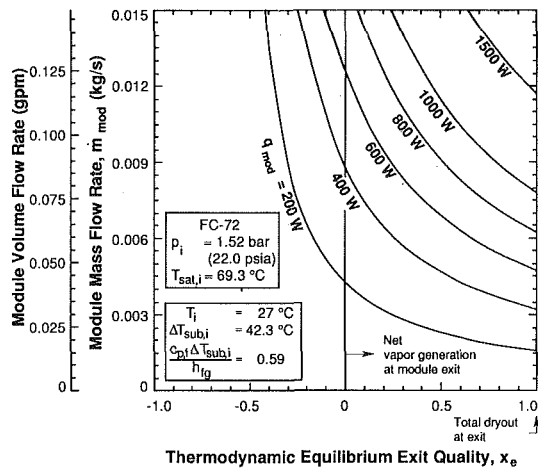


Fig. 4(a)

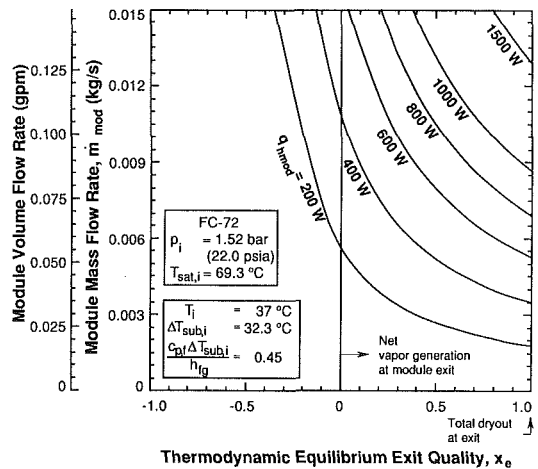


Fig. 4(b)

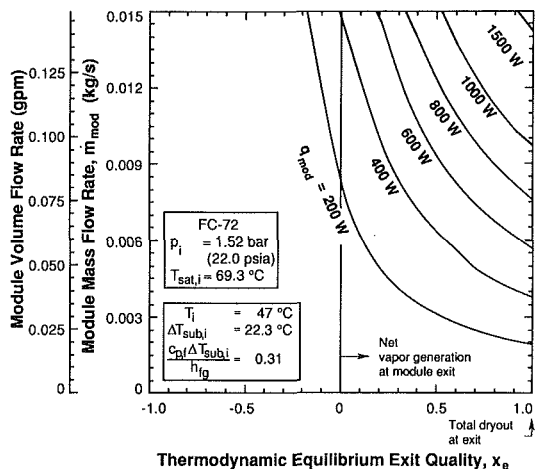


Fig. 4(c)

Fig. 4 Variation of module flow rate with thermodynamic equilibrium exit quality for different heat dissipation rates and inlet temperatures of (a) 27°C, (b) 37°C, and (c) 47°C

bubble layer was postulated to provide a greater opportunity for liquid to break through any coalescent vapor mass on the chip surface, thus delaying the transition to film boiling to higher heat fluxes. These phenomena were later explored experimentally by Gersey et al. (1992) and Willingham and Mudawar (1992) for a series of nine in-line chips. Highly subcooled

flow was observed to condense vapor bubbles a short distance downstream from each chip and increase CHF for each of the nine chips relative to saturated flow.

One measure of the extent of departure of a two-phase mixture from the saturated liquid state is the thermodynamic equilibrium quality. Maintaining the equilibrium quality at the module exit below zero helps reduce the danger of vapor exit from the module. Given the module flow rate, \dot{m}_{mod} , and module heat dissipation rate, q_{mod} , the thermodynamic equilibrium quality is determined from the relation

$$x_e = \frac{q_{mod}}{\dot{m}_{mod} h_{fg}} - \frac{c_{p,f} \Delta T_{sub,i}}{h_{fg}} \quad (1)$$

where $\Delta T_{sub,i}$ is the inlet subcooling.

Figures 4(a)–4(c) show variations of module flow rate with x_e for module heat dissipation rates ranging from 200 to 1500 W. Each of these figures shows increasing q_{mod} increases the flow rate required to prevent a net vapor generation at the module exit. Comparing the three figures reveals reducing $\Delta T_{sub,i}$ also increases the module flow rate requirements.

For conditions yielding $x_e \leq 0$, the module exit temperature can be calculated from a sensible heat balance on the entire module.

$$T_e - T_i = \frac{q_{mod}}{\dot{m}_{mod} c_{p,f}} \quad (2)$$

In designing and testing the clamshell module, upper limits for module heat dissipation were established by maintaining chip heat fluxes below the critical heat flux (CHF) corresponding to the subcooled conditions inside the cavity. First, CHF values for saturated boiling, $q''_{m,sat}$, were estimated using a theoretical model for pool boiling CHF developed by Zuber et al. (1961),

$$q''_{m,sat} = 0.131 \rho_g h_{fg} \left(\frac{\sigma g (\rho_f - \rho_g)}{\rho_g^2} \right)^{0.25} \quad (3)$$

The chip CHF values, q''_m , were then determined from Mudawar and Anderson's (1990) correlation for subcooled pool boiling CHF.

$$\frac{q''_m}{q''_{m,sat}} = 1 + 0.0643 \left(\frac{\rho_g}{\rho_f} \right)^{0.25} \frac{\rho_f c_{p,f} \Delta T_{sub}}{\rho_g h_{fg}} \quad (4)$$

Since ΔT_{sub} assumes different values depending upon the position of the individual chip relative to the inlet and outlet, a conservative (low) estimate for ΔT_{sub} was assumed by setting ΔT_{sub} equal to $\Delta T_{sub,e}$ the difference between the saturation temperature of 69.3°C, corresponding to an operating pressure of 1.52 bar, and module exit temperature, T_e , calculated using Eq. (2). Combining Eqs. (2) and (4) yields

$$q''_m = \frac{q''_{m,sat} \left[1 + 0.0643 \left(\frac{\rho_g}{\rho_f} \right)^{0.25} \frac{\rho_f c_{p,f} \Delta T_{sub,i}}{\rho_g h_{fg}} \right]}{1 + 0.0643 q''_{m,sat} \left(\frac{\rho_g}{\rho_f} \right)^{0.25} \frac{\rho_f N A_{chip}}{\rho_g h_{fg} \dot{m}_{mod}}} \quad (5)$$

where $\Delta T_{sub,i}$, N , and A_{chip} are the inlet subcooling, number of chips in the module, and chip area, respectively. Figure 5 shows CHF values predicted using Eqs. (3) and (5) and corresponding maximum values for module heat dissipation rate for inlet temperatures of 27, 37, and 47°C, assuming a module housing two circuit boards, each carrying sixteen 12.7×12.7 cm² chips, and neglecting the heat transfer contribution of the chip edges. Higher CHF values are predicted with increases in the module flow rate and/or decreases in the inlet temperature. Figure 5 also shows curves corresponding to $x_e = 0$ for the three inlet temperatures. A safety envelope, illustrated as an example for $T_i = 47^\circ\text{C}$ by the shaded area in Fig. 5, can be constructed by combining the limits of net vapor generation and CHF. A

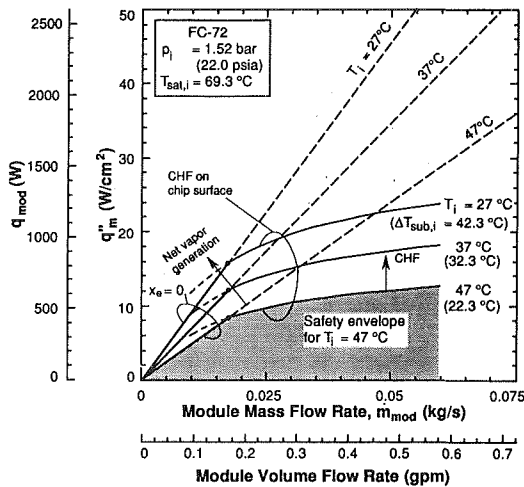


Fig. 5 Variation of chip CHF and module heat dissipation rate with flow rate for a module housing two circuit boards, each carrying sixteen $12.7 \times 12.7 \text{ mm}^2$ chips, for inlet temperatures of 27, 37, and 47°C

flow rate below that corresponding to the intersection between the two limits can result in vapor exiting the module at relatively low values of q_{mod} . In this case, the CHF limit is redundant since the module thermal requirements will not be met and because vapor may produce a global vapor dryout at fluxes much smaller than those predicted for an isolated chip in pool boiling. The CHF limit becomes the dominant safety criterion for flow rates exceeding those corresponding to the intersection point. Interestingly, increasing the module flow rate above the intersection value produces only modest increases in the CHF limit, whereas decreasing the inlet temperature greatly increases the CHF limit. These results demonstrate that, for a given inlet temperature, the module flow rate need not be much greater than the intersection value to avoid CHF. The safety envelope sets upper limits on q_{mod} of about 800, 1200, and 1550 W for inlet temperatures of 47, 37, and 27°C , respectively.

3 Experimental Methods

Clamshell Test Module. Flow visualization of the boiling process occurring within the module cavity played a key role in understanding the thermal behavior of the clamshell module. Of particular interest in the flow visualization studies was to ensure that no dryout occurred locally on the chip surfaces and to demonstrate that the vapor did not accumulate in the cavity during prolonged testing. Optical access to the module cavity required replacing cover *B*, along with circuit board *B*, with a clear cover made from Lexan. Protrusions identical in size and location to the chips in circuit board *A* were machined into the Lexan cover *B* to simulate the actual geometrical constraints which the heated chips in circuits board *A* would encounter. To block the coolant from flowing directly from the inlet slot to the outlet slot inside the cavity, the flow was diverted by a partition between the slots where the instrumentation wires were routed. Another modification, which was made to the original design shown in Fig. 3, was the substitution of the electrical connectors with sealed fittings for the instrumentation wires through plastic cover *B*. All parts of the test module were fabricated by a Mazatrol M-32 numerical machining center, which allowed for making of several duplicate modules with a high machining accuracy.

Sixteen simulated chips were mounted on circuit board *A*, each having a surface area of $1.27 \times 1.27 \text{ cm}^2$ and protruding 0.0254 cm (0.01 in) into the liquid. A thin film of RTV sealant applied along the edges of the chips precluded any significant

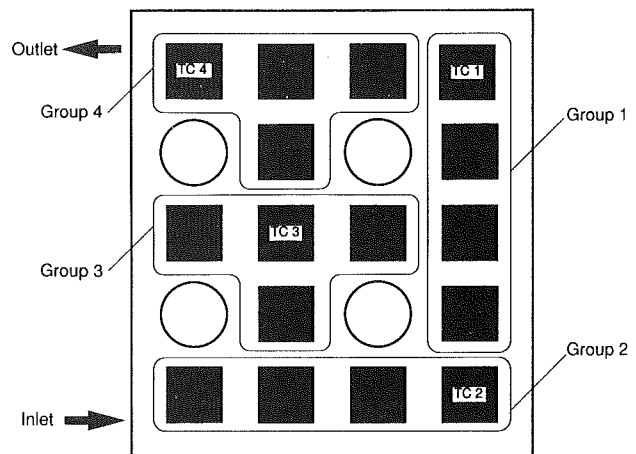


Fig. 6 Grouping and instrumentation of the simulated chips on circuit board *A*

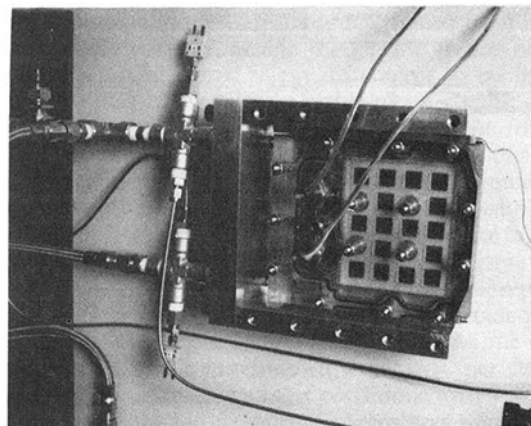


Fig. 7 Photograph of the clamshell test module mounted in the cardguide

boiling along the edges. The body of the chip was machined from an oxygen-free copper slab. A Chromel-Alumel thermocouple was embedded along the center of the copper slab 0.145 cm beneath the wetted surface. Silver soldered to the underside of the copper slab was a thick-film resistor which was used to supply heat to the chip. The chips were mounted on support platforms protruding from a base plate, both the platforms and base plate were made of G-7 fiberglass plastic. The entire assembly was covered with a G-7 lid which sealed the chip power leads and thermocouple wires and secured the chips in position. As shown in Fig. 6, every four of the chips were electrically connected in series, a total of four groups, and the four groups were then wired in parallel and connected to an external 240-Vac auto-transformer. Thus, one voltage transducer and four current transducers were sufficient to monitor the power dissipated by each group. One chip in each group was instrumented with a thermocouple as marked in Fig. 6.

In order to closely simulate the placement of the clamshell module in the enclosure, a cardguide resembling a slice of the avionic enclosure was constructed. The cardguide included two wedge clamps and a backboard where the fluid couplers were mounted. Figure 7 shows the clamshell test module mounted in the cardguide.

Flow Loop. Figure 8 shows a schematic diagram of the flow loop which was used to condition the coolant for thermal testing of the module. The coolant was circulated through the loop by a magnetically-coupled centrifugal pump. Coolant

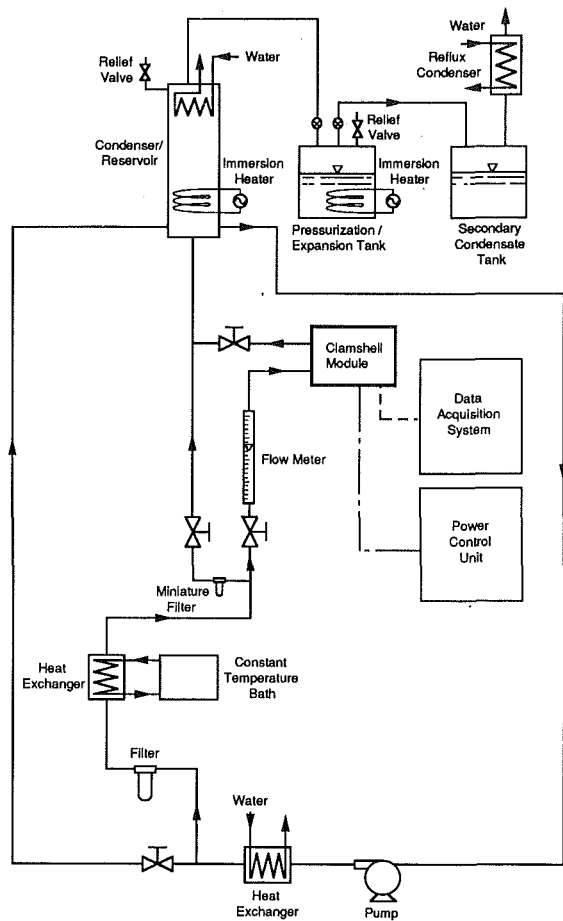


Fig. 8 Two-phase flow loop

temperature at the module inlet was regulated by a water-cooled heat exchanger and fine tuned by a constant temperature bath. Pressure was controlled to within ± 0.0103 bar (± 0.15 psia) by a pressurization tank and a condenser submerged in the condenser/reservoir shown in Fig. 8. The coolant was carefully filtered upstream of the module inlet disconnect coupler using two 5-micron filters.

Because the two-phase loop was originally designed for experiments requiring large flow rates, most of the coolant flow had to be bypassed to accommodate the clamshell module's low flow rates. The flow was bypassed at two locations and the module fluid was routed into a flow meter before entering the module. An Omega FL-115 rotameter was used to measure flow rates in the range 5.0×10^{-7} to 3.17×10^{-5} m³/s. Regulating valves were located in the two by-pass lines, upstream of the flow meter and just downstream of the module outlet, to fine tune pressure and flow rate at the module inlet. After exiting the module, the module fluid recombined with the bypassed flow and the mixture was returned to the condenser/reservoir.

Thermocouples were inserted in the lines just upstream and downstream of the clamshell module to measure liquid temperatures at the respective locations. An absolute pressure transducer with a range of 0 to 10.3 bar measured the module inlet pressure while pressure difference across the module was measured using a differential pressure transducer with a range of 0 to 3.45 bar.

Operating Procedure. Prior to each test, the system was deaerated to remove any noncondensable gases from the fluid. Deaeration was accomplished by heating the fluid to its saturation temperature, using the immersion heaters in the condenser/reservoir and the pressurization/expansion tank, to

force the noncondensable gases, mixed with some FC-72 vapor, into the secondary condensate tank and then to the water-cooled reflux condenser. The FC-72 vapor was recaptured by condensation as the noncondensable gases escaped to the ambient. After approximately ten minutes, the valve connecting the pressurization/expansion tank to the secondary condensate tank was closed and the system was ready for testing.

The system pressure was maintained by the condenser/reservoir and the pressurization/expansion tank located in the main flow loop. Pressure was controlled by regulating the energy from the immersion heater in the pressurization/expansion tank and the rate of cold water flow into the submerged condenser in the condenser/reservoir. The cold water flow in the submerged condenser was controlled by a solenoid valve actuated by the data acquisition system.

To obtain boiling data, the power to the chips was increased in small increments while maintaining the module inlet pressure and inlet temperature constant. Using a Keithley 500 data acquisition system interfaced to a Compaq computer, a data point was taken once the four instrumented chips attained steady-state temperatures. Steady state was assumed when twenty consecutive readings had a standard deviation less than 0.10°C . Testing was terminated when excessive vapor buildup was observed inside the module cavity for fear of damaging the circuit board. It should be noted that critical heat flux was never reached during any of the tests performed on the module during this study since the chip heat fluxes were maintained with the safety envelope determined from Fig. 5.

Experimental Uncertainty. Experimental uncertainties resulted from errors in the various instruments used in the measurements. The maximum uncertainty associated with each thermocouple reading was estimated to be less than 0.2°C . The voltage and current transducers were carefully calibrated, and the maximum error in the power reading was estimated to be ± 5.7 percent at 160 W per board (half module) decreasing to ± 3.6 percent at 400 W per board. A one-dimensional heat conduction model of the clamshell determined that the largest heat loss from the chips was 0.8 percent; thus, no adjustments were made to the electrically measured chip heat flux. Other experimental uncertainties include flow meter readings, ± 1.6 percent, and readings from the two pressure transducers, ± 0.0103 bar (± 0.15 psi).

3 Results and Discussion

Boiling Curves. The test module, referred to hereafter as *half-module*, was tested both at twice and one-half the inlet operating pressure of 1.52 (22.0 psia) during a full cycle of engagement and disengagement in the card guide. There were no signs of Fluorinert spillage or air inclusion at the couplers or the module seals. The primary objective of the thermal tests was to determine the minimum values for subcooling and coolant flow rate that would safely dissipate the module heat and prevent vapor exit from the module.

Tests were performed by supplying equal power to all the chips. The coolant, FC-72, was supplied at 1.52 bar, corresponding to a saturation temperature of 69°C , and $\Delta T_{\text{sub},i}$ of 22.3, 32.3, and 42.3°C (which correspond to $T_i = 47, 37,$ and 27°C , respectively). The trajectories of bubbles emanating from the chips, and the waviness induced by gradients in the index of refraction of the liquid proved the coolant circulated adequately within the cavity prior to exiting the module with the exception of the two corner regions away from the inlet and exit ports. In all of these tests, chips in the right corner of circuit board A, Fig. 6, nucleated first. The same chips produced larger amounts of vapor in the nucleate boiling regime than the remaining chips. This may be the result of a relatively poor liquid circulation (i.e., smaller single-phase heat transfer

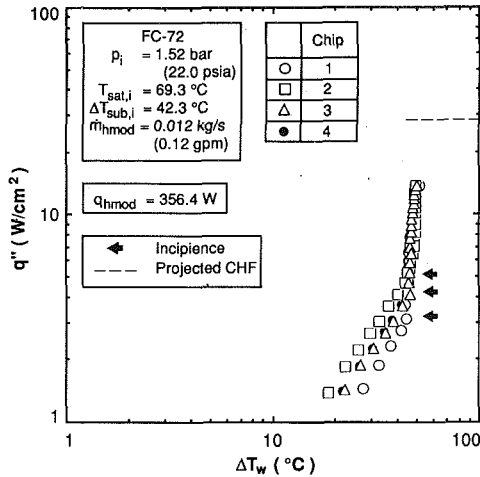


Fig. 9(a)

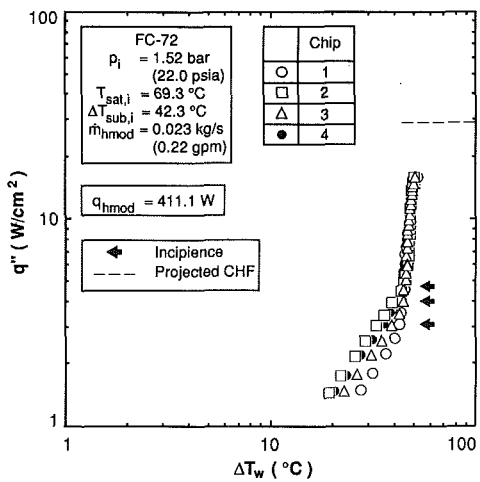


Fig. 9(b)

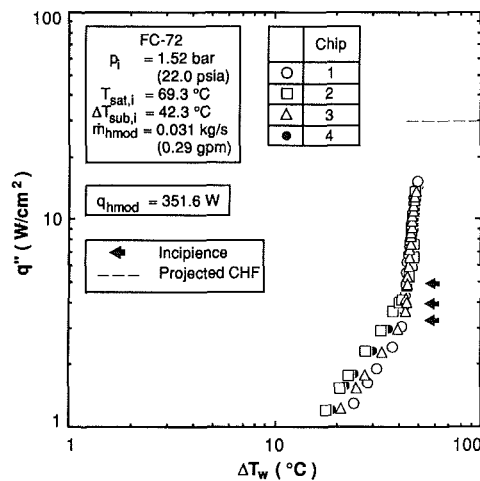


Fig. 9(c)

Fig. 9 Boiling curves for the four instrumented chips at $\Delta T_{sub,i} = 42.3$ °C and half-module flow rates of (a) 0.012 kg/s, (b) 0.023 kg/s, and (c) 0.031 kg/s

coefficient) in the corner region of the module causing boiling incipience at relatively low heat fluxes.

Figures 9(a)–9(c) show boiling curves for the four instrumented chips corresponding to $\Delta T_{sub,i} = 42.3$ °C and flow rates

Table 2 Maximum values of heat dissipation rate, chip temperature, guide rib temperature, and pressure drop across the module measured for the various test conditions

\dot{m}_{hmod} kg/s	T_i °C	Max q_{hmod} W	Max T_i °C	Max T_2 °C	Max T_3 °C	Max T_4 °C	Max T_{guide} °C	Max T_e °C	Δp bar (psi)	
1.22×10^{-2}	27	356.4	78.7	76.5	76.9	77.5	46.3	49.6	0.050 (0.72)	
		369.7	78.9	76.8	77.1	77.6	45.7	46.1	0.070 (1.01)	
		402.7	79.6	77.2	77.5	77.9	47.7	44.1	0.109 (1.58)	
		2.32 $\times 10^{-2}$	411.1	79.2	77.0	77.4	77.8	46.3	41.4	0.149 (2.16)
		2.68 $\times 10^{-2}$	403.2	78.8	76.5	76.9	77.0	47.3	39.6	0.202 (2.93)
		3.07 $\times 10^{-2}$	351.6	76.4	75.1	75.4	75.1	43.3	36.9	0.259 (3.75)
1.22×10^{-2}	37	254.6	76.2	74.3	74.3	75.2	51.4	51.4	0.050 (0.72)	
		271.0	76.3	74.3	74.5	75.3	51.6	47.4	0.112 (1.62)	
		3.07 $\times 10^{-2}$	287.8	75.6	72.9	73.5	74.1	51.1	44.2	0.267 (3.87)
1.22×10^{-2}	47	221.6	76.0	74.6	74.6	75.2	57.1	58.7	0.054 (0.79)	
		210.6	74.8	74.0	74.0	74.9	56.7	54.8	0.117 (1.69)	
		3.07 $\times 10^{-2}$	261.2	74.7	73.1	73.3	73.6	56.6	53.3	0.290 (4.20)

of 0.012, 0.023, and 0.031 kg/s, respectively. Given in each of these three figures is the “half-module” flow rate, \dot{m}_{hmod} , “half-module” heat dissipation rate, q_{hmod} , at which the test was terminated, and the CHF limit determined from Eqs. (3) and (5). These curves illustrate the general trends observed with all the module tests. Slight differences in cooling performance were observed in the single-phase regime. Chip 1 had the lowest single-phase heat transfer coefficient, followed, in order, by Chips 3, 4, and 2. The lowest single-phase heat transfer coefficient (Chips 1) is attributed to poor liquid access to the upper right corner region. Once in the nucleate boiling regime, the four chips showed virtually no difference in surface temperature, a behavior characteristic of this regime due to the weak influence of fluid motion on the nucleation process.

Table 2 gives maximum values for the important thermal parameters of the test module. The table shows the desired cooling rate of 250 W per board (i.e., 500 W per clamshell module) was exceeded for all test conditions with $T_i = 27$ and 37 °C, and the chip and guide rib temperatures were less than 80 and 60 °C, respectively. A cooling rate of 411.1 W per board was achieved with a flow rate of only 0.023 kg/s (0.221 gpm) and pressure drop of 0.149 bar (2.16 psi)

Subcooling. Supplying the coolant at a temperature well below its boiling temperature corresponding to the inlet pressure was observed to greatly reduce bubble size and helped accelerate the condensation of vapor bubbles within the module cavity. When testing the module at the coolest inlet condition, $\Delta T_{sub,i} = 42.3$ °C, the vapor from the chips quickly condensed before reaching the surrounding chips. With flow rates below 0.027 kg/s (0.255 gpm), some vapor began to coalesce into small pockets at the top of the module cavity for chip heat fluxes of 9.32 to 12.42 W/cm², and at 11.18 to 13.66 W/cm² (i.e., 288 to 352 W per half module), the vapor pockets grew steadily yet slowly. Higher chip heat fluxes caused the vapor accumulation to accelerate until the lower edge of the coalescent vapor mass was level with the opening of the outlet port. Once this occurred, small amounts of vapor were observed exiting the outlet port. The fluid level then became stable even with further power increases, and vigorous boiling was observed on the top row of chips. Nevertheless, chip dryout was not encountered because the chips were located below the module outlet port. Vapor accumulation was also observed at $\Delta T_{sub,i} = 22.3$ and 32.3 °C but at lower heat fluxes. Figure 10 summarizes the various boiling and stratification regimes observed in the module cavity. These regimes demonstrate maintaining $x_2 \leq 0$ does not preclude phase separation (stratification) in the module cavity and subcooling is the most effective means for preventing stratification.

Coalescence into vapor pockets at the top of the module was completely inhibited, at all the tested heat fluxes, at $\Delta T_{sub,i} = 42.3$ °C and coolant flow rates above 0.027 kg/s (0.255

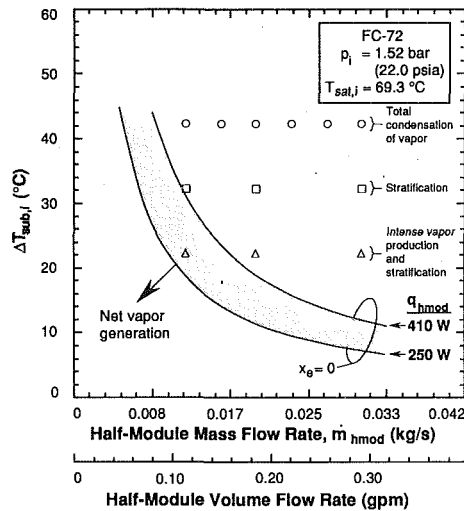


Fig. 10 Summary of boiling and stratification regimes observed in the cavity of the clamshell test module at the highest heat dissipation rate for each test condition

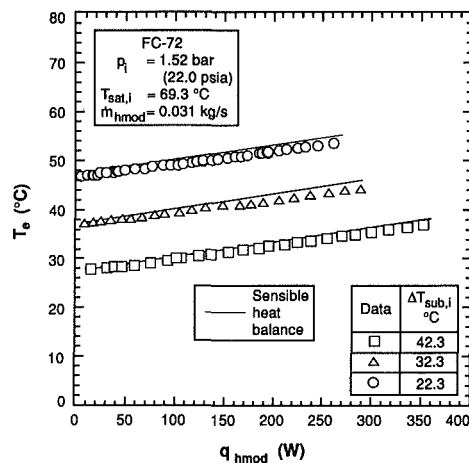


Fig. 11 Variation of the measured coolant exit temperature with rate of heat dissipation compared to predictions of sensible heat balance on the simulated half-module

gpm). This feature greatly simplifies coolant conditioning external to the clamshell modules in an avionic enclosure by employing a basic single-phase loop consisting of a only a pump and liquid-to-air heat exchanger. Rapid condensation of bubbles immediately following departure from the surface also greatly reduces the danger of phase separation during the large G-field fluctuations of military aircraft. Thus, it is recommended that inlet conditions be set closed to $\Delta T_{sub,i} = 42.3^\circ\text{C}$ and flow rates exceeding 0.027 kg/s (0.255 gpm) per board (or 0.054 kg/s , 0.51 gpm , per clamshell module).

Module Exit Temperature. Figure 11 shows the outlet temperatures measured experimentally are very close to the values predicted from a simple sensible heat balance, Eq. (6), on the simulated half-module. Three sets of data are shown for the three tested values of subcooling. The data follow lines with fairly equal slopes with increasing power dissipation. Figure 11 lends further support to the observation of complete bubble condensation prior to coolant exit from the module.

Pressure Drop Across the Test Module. Yet, another proof of the effectiveness of bubble condensation is the insensitivity of the measured pressure drop to variations in the total power dissipation. Figure 12 shows, at $\Delta T_{sub,i} = 42.3^\circ\text{C}$, the pressure

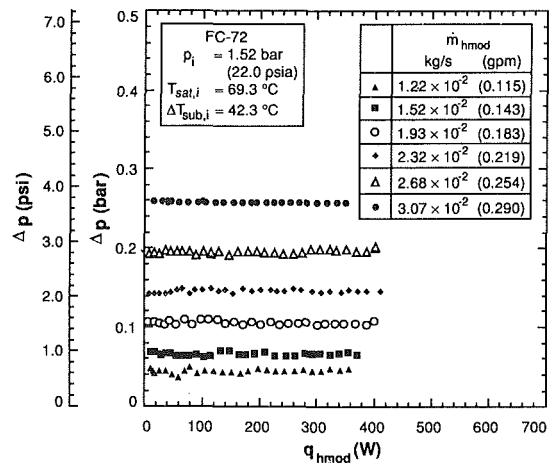


Fig. 12 Variation of pressure drop with heat dissipation rate for different flow rates

drop was virtually constant for each of six flow rates between 0.012 and 0.031 kg/s . This indicates that, despite the occasional accumulation of vapor along the upper edge of the module, virtually all of the vapor condensed prior to exiting the module since any release of vapor through the outlet port would have created a measurable increase in pressure drop. Figure 12 also shows pressure drop across the module was very small due to a combination of the relatively small flow coefficient of the couplers used, the unrestricted coolant flow within the module cavity, and the aforementioned condensation of the vapor prior to exiting the module. These low pressure drop characteristics are of paramount importance in demonstrating the feasibility of the *BTPFL-C1* module since these characteristics made possible operation with a relatively small cavity pressure and precluded the need for thick module walls. Structural calculations revealed that, with this pressure, only one support screw, rather than the four shown in Fig.3, should be adequate for supporting the module.

4 Conclusions

This study involved the design, fabrication, and testing of a new building block for future high-flux aircraft avionics using phase-change immersion cooling. Key conclusions from the study are as follows:

(1) The required heat dissipation of 250 W per board was exceeded at all the tested flow rates with inlet temperatures of 27 and 37°C . The tests exceeded 350 W per board for a coolant flow rate and pressure drop of 0.012 kg/s (0.11 gpm) and 0.050 bar (0.72 psi), respectively. At 0.023 kg/s (0.221 gpm) and 0.149 bar (2.16 psi), heat dissipation of more than 410 W per board was exceeded while maintaining stable and repeatable chip temperatures. Since CHF was the dominant criterion in the module's safety envelope, the present results prove that, even if the coolant flow rate is doubled for a full clamshell module, the flow rate and pressure drop required to dissipate in excess of 820 W would still be very small. This cooling rate is well above the requirements for avionic modules proposed for the next two decades.

(2) Reducing the inlet temperature greatly reduced bubble size, and helped ensure complete condensation of the bubbles within the module cavity. Thus, with a high degree of subcooling, coolant conditioning external to module can be greatly simplified by employing a basic single-phase liquid loop consisting of only a pump and liquid-to-air heat exchanger.

(3) A combination of the relatively small pressure drop of the quick disconnect couplers used and unrestricted coolant flow within the module cavity produced very small pressure

drops. The pressure drop remained constant with increasing power dissipation due to the complete condensation of vapor prior to exiting the module.

(4) Despite the coolant flow being undirected within the module cavity, the heat sources acquired fairly uniform temperatures at equal powers. Only slight nonuniformities were measured in the single-phase regime, especially with the heat sources located in the corners farthest from the inlet.

(5) The chip and guide rib temperatures were maintained below 80 and 60°C respectively, for all the tested conditions, thus satisfying key thermal requirements of future advanced aircraft.

Acknowledgment

This work was supported by the Naval Air Warfare Center, Aircraft Division, Indianapolis, under contract N00163-91-C0222.

References

- Anderson, T. M., and Mudawar, I., 1989, "Microelectronic Cooling by Enhanced Pool Boiling of a Dielectric Fluorocarbon Liquid," *ASME Journal of Heat Transfer*, Vol. 111, pp. 752-759.
- Barwick, M., Midkoff, M., and Seals, D., 1991, "Liquid Flow-Through Cooling for Avionics Applications," *Proc. IEEE 1991 National Aerospace and Electronics Conf.*, (NAECON), Vol. 1, Dayton, Ohio, pp. 227-230.
- Bowers, M. B., and Mudawar, I., 1994, "High Flux Boiling in Low Flow Rate, Low Pressure Drop Mini-Channel and Micro-Channel Heat Sinks," *Int. J. Heat Mass Transfer*, Vol. 37, pp. 321-332.
- Galloway, J. E., and Mudawar, I., 1992, "Critical Heat Flux Enhancement by Means of Liquid Subcooling and Centrifugal Force Induced by Flow Curvature," *Int. J. Heat Mass Transfer*, Vol. 35, pp. 1247-1260.
- Gersey, C. O., Willingham, T. C., and Mudawar, I., 1992, "Design Parameters and Practical Considerations in the Two-Phase Forced-Convection Cooling of Multi-Chip Modules," *ASME JOURNAL OF ELECTRONIC PACKAGING*, Vol. 114, pp. 280-289.
- Grimley, T. G., Mudawar, I., and Incropera, F. P., 1988, "Limits to Critical Heat Flux Enhancement in a Liquid Film Falling over a Structure Surface Which

Simulates a Microelectronic Chip," *ASME Journal of Heat Transfer*, Vol. 110, pp. 535-538.

Ma, C. F., and Bergles, A. E., 1983, "Boiling Jet Impingement Cooling of Simulated Microelectronic Chips," *Heat Transfer in Electronic Equipment*, ASME HTD, Vol. 28, pp. 5-12.

Mackowski, M., 1991, "Requirements for High Flux Cooling of Future Avionics Systems," SAE Paper 912104.

Maddox, D. E., and Mudawar, I., 1989, "Single and Two-Phase Convective Heat Transfer from Smooth and Enhanced Microelectronics Heat Sources in a Rectangular Channel," *ASME Journal of Heat Transfer*, Vol. 111, pp. 1045-1052.

Monde, M., and Katto, Y., 1978, "Burnout in a High Heat-Flux Boiling System with an Impinging Jet," *Int. J. Heat Mass Transfer*, Vol. 21, pp. 295-305.

Mudawar, I., and Anderson, T. M., 1990, "Parametric Investigation into the Effects of Pressure, Subcooling, Surface Augmentation and Choice of Coolant on Pool Boiling in the Design of Cooling Systems for High-Power Density Chips," *ASME JOURNAL OF ELECTRONIC PACKAGING*, Vol. 112, pp. 375-382.

Mudawar, I., and Maddox, D. E., 1989, "Critical Heat Flux in Subcooled Flow Boiling of Fluorocarbon Liquid on a Simulated Electronic Chip in a Vertical Rectangular Channel," *Int. J. Heat Mass Transfer*, Vol. 32, pp. 379-394.

Mudawar, I., and Maddox, D. E., 1990, "Enhancement of Critical Heat Flux from High Power Microelectronic Heat Sources in a Flow Channel," *ASME JOURNAL OF ELECTRONIC PACKAGING*, Vol. 112, pp. 241-248.

Nakayama, W., Nakajima, T., and Hirasawa, S., 1984, "Heat Sink Studs Having Enhanced Boiling Surfaces for Cooling of Microelectronic Components," ASME Paper 84-WA/HT-89.

Phillips, R. J., 1988, "Forced-Convection, Liquid-Cooled, Microchannel Heat Sinks", M.I.T. Lincoln Laboratory Technical Report 787.

Tuckerman, D. B., and Pease, R. F., 1981, "Ultrahigh Thermal Conductance Microstructures for Cooling Integrated Circuits," *Proc. 32nd Electronic Components Conf.*, pp. 145-149.

Wadsworth, D. C., and Mudawar, I., 1990, "Cooling of a Multichip Electronic Module by Means of Confined Two-Dimensional Jets of Dielectric Liquid," *ASME JOURNAL OF HEAT TRANSFER*, Vol. 112, pp. 891-898.

Wadsworth, D. C., and Mudawar, I., 1992, "Enhancement of Single-Phase Heat Transfer and Critical Heat Flux from an Ultra-High-Flux Simulated Microelectronic Heat Source to a Rectangular Impinging Jet of Dielectric Liquid," *ASME Journal of Heat Transfer*, Vol. 114, pp. 764-768.

Willingham, T. C., and Mudawar, I., 1992, "Forced-Convection Boiling and Critical Heat Flux from a Linear Array of Discrete Heat Sources," *Int. J. Heat Mass Transfer*, Vol. 35, pp. 2879-2890.

Zuber, N., Tribus, M., and Westwater, J. W., 1961, "The Hydrodynamic Crisis in Pool Boiling of Saturated and Subcooled Liquids," *Int. Developments in Heat Transfer*, Part 2, ASME, pp. 230-236.